Molecular Shape and Solvation of the Lacunar, Saddle-Shaped, and Planar Metal Cyclidene Complexes: Molecular Dynamics Studies

Elena V. Rybak-Akimova,*,†,‡ Krzysztof Kuczera,*,‡,§ Gouri S. Jas,‡,§ Yanpei Deng,‡ and Daryle H. Busch*,‡

Departments of Chemistry and Biochemistry, University of Kansas, Lawrence, Kansas 66045, and Department of Chemistry, Tufts University, Medford, Massachusetts 02155

Received April 27, 1999

Molecular dynamics simulations have been used to study the three-dimensional distribution of methanol solvent molecules around three cobalt(II) cyclidene complexes differing in details of their ligand structures. The ligands are a planar unbridged 14-membered macrocycle in Co([14]Cyc), a saddle-shaped unbridged 16-membered macrocycle in Co([16]Cyc), and a lacunar bridged 16-membered macrocycle in Co(C6[16]Cyc). All three complexes contain five-coordinate cobalt(II) with the metal ion bound to four nitrogen donor atoms from the macrocycle and one nitrogen donor from an axial methylimidazole. Distinctly different solvation patterns are exemplified for the three complexes by the positions of the maximum in the Co−O pair distribution function (at r(Co−O) = 2.5, 3.7, and 4.5 Å for Co([14]Cyc), Co([16]Cyc), and Co(C6[16]Cyc), respectively) and by the number of methanol molecules within the macrocyclic cleft (1.5, 0.7, and 0.4 molecules at a Co−O distance of 5.25 Å in the "cavity", respectively). Analysis of the anisotropic solvent structure reveals the presence of a methanol molecule directly above the cobalt(II) center, at a distance of ca. 2.5 Å, for planar Co([14]Cyc), and the absence of solvent from such close proximity to the metal ion for the remaining complexes. The bridge further protects the sides of the cavity from the solvent. The width of an empty cavity of Co(C6[16]Cyc) shrinks by 0.3 Å in methanol solution, as compared to vacuum simulations. These results confirm the experimentally based (decrease in absolute value of enthalpies and entropies of dioxygen binding) suggestion that extensive solvation of the cobalt(II) center reduces its accessibility to incoming small molecules.

Introduction

Building superstructures around the metal ions has become one of the popular motives in the design of novel coordination compounds, with numerous successful implementations to macrocyclic porphyrin and non-porphyrin complexes. [1,2] The approach originates from the chemistry of synthetic dioxygen carriers, where the steric bulk around the metal center served at least two purposes: (1) to protect the dioxygen adduct from autoxidation via μ-oxo dimer formation and (2) to prevent the binding of large base or solvent molecules at the sixth vacant coordination site of the metal ion, leaving it available for O_2 binding. This paradigm of steric protection at the metal coordination site has been extended to reversible binding and activation of various small molecules. Recent applications include (but are not limited to) binding and activation of dioxygen and peroxide with sterically hindered non-heme iron complexes[3−6] and copper(I) complexes;[7,8] shape-selective oxidation of substrates catalyzed by superstructured metalloporphyrins;[9] dinitrogen fixation using molybdenum complexes with tripodal ligands bearing bulky substituents;[10] etc. In general, a sterically hindered metal coordination site facilitates discrimination between other ligands ("guests") of different sizes and shapes and protection of reactive coordinated species. The sterically protected metal coordination sites are also very important in the functioning of naturally occurring metalloproteins.[11]

The expected "side effect" of the superstructure encompassing the small-molecule binding site, the decrease in the binding rates and dioxygen affinities with an increasing extent of steric hindrance, has been observed for many porphyrin and non-porphyrin complexes.[2,12] This effect, which is primarily entropic in nature, can be easily rationalized in terms of restricted number of possible orientations and trajectories of a small ligand that allow access into the cavity. In other words, the superstructure will "overprotect" the binding site; it not only prevents the binding of undesirable components of the reaction mixture but also hinders the binding of the desired substrate. The differences in size, shape, and solvent affinity between available small substrates (e.g., O_2) and the competing solvent or base molecules (e.g., methanol, *N*-methylimidazole, and Cl^-) open the way for fine-tuning the binding characteristics of the lacunar complexes by varying the size, shape, and atomic composition of the cavity.

† Tufts University.
‡ University of Kansas, Department of Chemistry.
§ University of Kansas, Department of Biochemistry.

(1) Busch, D. H.; Alcock, N. W. *Chem. Rev.* **1994**, *94*, 585−623.
(2) Momenteau, M.; Reed, C. A. *Chem. Rev.* **1994**, *94*, 659−698.
(3) Feig, A. L.; Lippard, S. J. *Chem. Rev.* **1994**, *94*, 759−805.
(4) Que, L., Jr.; Dong, Y. *Acc. Chem. Res.* **1996**, *29*, 190.
(5) Que, L., Jr. *J. Chem. Soc., Dalton Trans.* **1997**, 3933−3940.
(6) Hayashi, Y.; Suzuki, M.; Uehara, A.; Mizutani, Y.; Kitagawa, T. *Chem. Lett.* **1992**, 91.
(7) Uozumi, K.; Hayashi, Y.; Suzuki, M.; Uehara, A. *Chem. Lett.* **1993**, 963.
(8) Tolman, W. B. *Acc. Chem. Res.* **1997**, *30*, 227−237.
(9) Suslick, K. S.; van Deusen-Jeffries, S. *Compr. Supramol. Chem.* **1996**, *5*, 141.
(10) Schrock, R. R. *Acc. Chem. Res.* **1997**, *30*, 9−16.
(11) Bertini, I.; Gray, H. B.; Lippard, S. J.; Valentine, J. *Bioinorganic Chemistry*; University Science Books: Mill Valley, CA, 1994.
(12) Busch, D. H.; Jackson, P. J.; Kojima, M.; Chmielewski, P.; Matsumoto, N.; Stevens, J. C.; Wu, W.; Nosco, D.; Herron, N.; Ye, N.; Warburton, P. R.; Masarwa, M.; Stephenson, N. A.; Christoph, G.; Alcock, N. W. *Inorg. Chem.* **1994**, *33*, 910−923.

10.1021/ic9904485 CCC: $18.00
Published on Web 06/24/1999

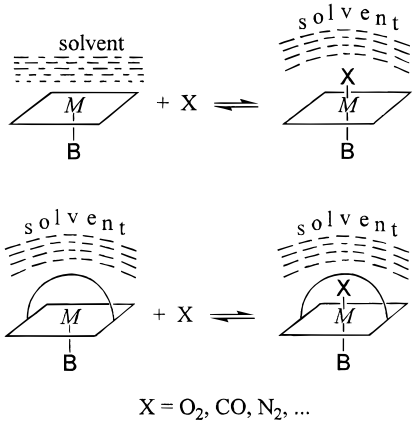

Figure 1. Nonspecific "solvent shielding" of the coordination site in non sterically hindered complexes, as compared to the "bridge shielding" in the corresponding lacunar complexes (suggested by Collman and co-workers[21]).

This approach allowed us, for example, to accomplish fast, low-barrier oxygenation at a vacant cobalt(II) coordination site in bridged cyclidene complexes[13,14] (the second-order rate constants on the order of 10^8 M^{-1} s^{-1} are comparable to those for natural oxygen carriers).

Surprising results were obtained when the reactivities in noncoordinating solvents of lacunar complexes and their unbridged analogues were compared. In such media, solvent molecules are not expected to compete with the small ligand molecules for the binding sites, and steric hindrance around the coordination site was not expected to lead to enhanced reactivity. The opposite was expected, a decrease in reactivity for the lacunar (sterically hindered) complexes when compared to their unbridged analogues. Experimental studies on dioxygen and carbon monoxide binding to "flat" and sterically hindered porphyrins gave contradictory results. In some cases, "flat" porphyrins formed stronger O_2 or CO adducts than their "protected" derivatives, due to faster binding rates.[15−20] In other cases, however, the opposite trend was observed: the sterically hindered porphyrins outperformed their "flat" (unsubstituted) analogues in small-molecule binding rates and the stabilities of the adducts formed.[21−23] A nonspecific "solvent shielding" of the metal coordination site was suggested as a possible explanation for this counterintuitive effect[21,22] (Figure 1). Recently, we observed ca. 100 times faster oxygenation of the bridged cobalt(II) complexes with pentadentate Schiff base ligands, as compared to the analogous parent unbridged compounds.[24] A smaller but measurable effect was also found in the oxygen binding to bridged versus unbridged cobalt(II) cyclidenes.[14] The "solvent shielding" hypothesis offers a reasonable explanation for this accumulating set of observations. The hypothesis itself, however, has not previously been justified. The analysis of the solvent structure around the metal site in coordination compounds of different shapes is reported here, and the results provide important insights into the reactivities of such complexes in solution.

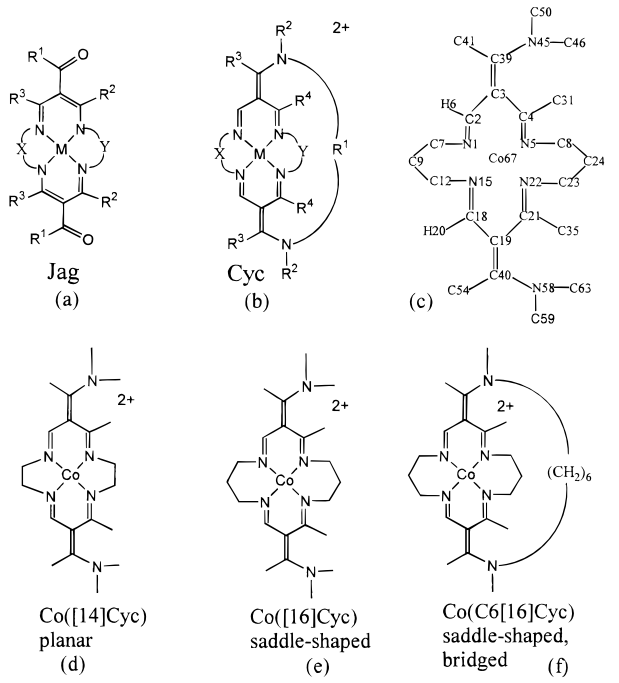

Figure 2. Macrocyclic complexes: (a) general structure of Jäger complexes; (b) general structure of cyclidene complexes; (c) atom-numbering scheme for macrocyclic framework adopted in modeling studies; (d−f) cyclidene complexes selected for molecular dynamics simulations.

Cyclidene complexes (Figure 2) provide a perfect opportunity to analyze the influence of molecular shape and superstructure on solvation of the metal center. X-ray crystallographic studies[1,12,25] revealed that the 16-membered macrocyclic ring in cyclidenes folds and adopts a deep saddle-shaped conformation in unbridged complexes, as well as in bridged derivatives (Figure 3). In unbridged compounds, one site at the metal ion is sterically protected by the "walls" of the cavity, while in bridged complexes the protective walls are still in place but additional protection is provided by the "roof" over the cleft (the bridge). In contrast, the 14-membered macrocyclic ring preferentially exists in a flat or "open" conformation (Figure 3), and the metal ion in its square-planar coordination environment is fully exposed to solvent molecules and other components of the reaction mixture. A comparative study of these systems allows us to elucidate the roles of different structural components ("walls" and "roof") in shielding the metal ion from the solvent.

In the absence of direct experimental methods capable of displaying the spatial distribution of solvent molecules around the metal center within the bulky ligands, molecular dynamics simulations can be used to obtain this information. Molecular dynamics and Monte Carlo simulations proved to be valuable

(13) Rybak-Akimova, E. V.; Masarwa, M.; Marek, K.; Warburton, P. R.; Busch, D. H. *Chem. Commun.* **1996**, 1451−1452.
(14) Rybak-Akimova, E. V.; Marek, K.; Masarwa, M.; Busch, D. H. *Inorg. Chim. Acta* **1998**, *270*, 151−161.
(15) Linard, J. E.; Ellis, P. E., Jr.; Budge, J. R.; Jones, R. D.; Basolo, F. *J. Am. Chem. Soc.* **1980**, *102*, 1896.
(16) Hashimoto, T.; Dyer, R. L.; Crossley, M. J.; Baldwin, J. E.; Basolo, F. *J. Am. Chem. Soc.* **1982**, *104*, 2101.
(17) Traylor, T. G.; Mitchell, M. J.; Tsuchiya, S.; Campbell, D. H.; Stynes, D. V.; Koga, N. *J. Am. Chem. Soc.* **1981**, *103*, 5234.
(18) Traylor, T. G.; Tsuchiya, S.; Campbell, D. H.; Mitchell, M. J.; Stynes, D. V.; Koga, N. *J. Am. Chem. Soc.* **1985**, *107*, 604.
(19) Traylor, T. G.; Koga, N.; Deardurff, L. A. *J. Am. Chem. Soc.* **1985**, *107*, 6504.
(20) David, S.; James, B. R.; Dolphin, D.; Traylor, T. G.; Lopez, M. A. *J. Am. Chem. Soc.* **1994**, *116*, 6.
(21) Collman, J. P.; Brauman, J. I.; Iverson, B. L.; Sessler, J. L.; Morris, R. M.; Gibson, Q. H. *J. Am. Chem. Soc.* **1983**, *105*, 3052−3064.
(22) Collman, J. P.; Brauman, J. I.; Doxsee, K. M.; Halbert, T. R.; Hayes, S. E.; Suslick, K. S. *J. Am. Chem. Soc.* **1978**, *100*, 2761−2766.
(23) Collman, J. P.; Zhang, X. M.; Wong, K.; Brauman, J. I. *J. Am. Chem. Soc.* **1994**, *116*, 6245.
(24) Rybak-Akimova, E. V.; Otto, W.; Deardorf, P.; Roesner, R.; Busch, D. H. *Inorg. Chem.* **1997**, *36*, 2746−2753.
(25) Alcock, N. W.; Lin, W.-K.; Jircitano, A.; Mokren, J. D.; Corfield, P. W. R.; Johnson, G.; Novotnak, G.; Cairns, C.; Busch, D. H. *Inorg. Chem.* **1987**, *26*, 440−452.

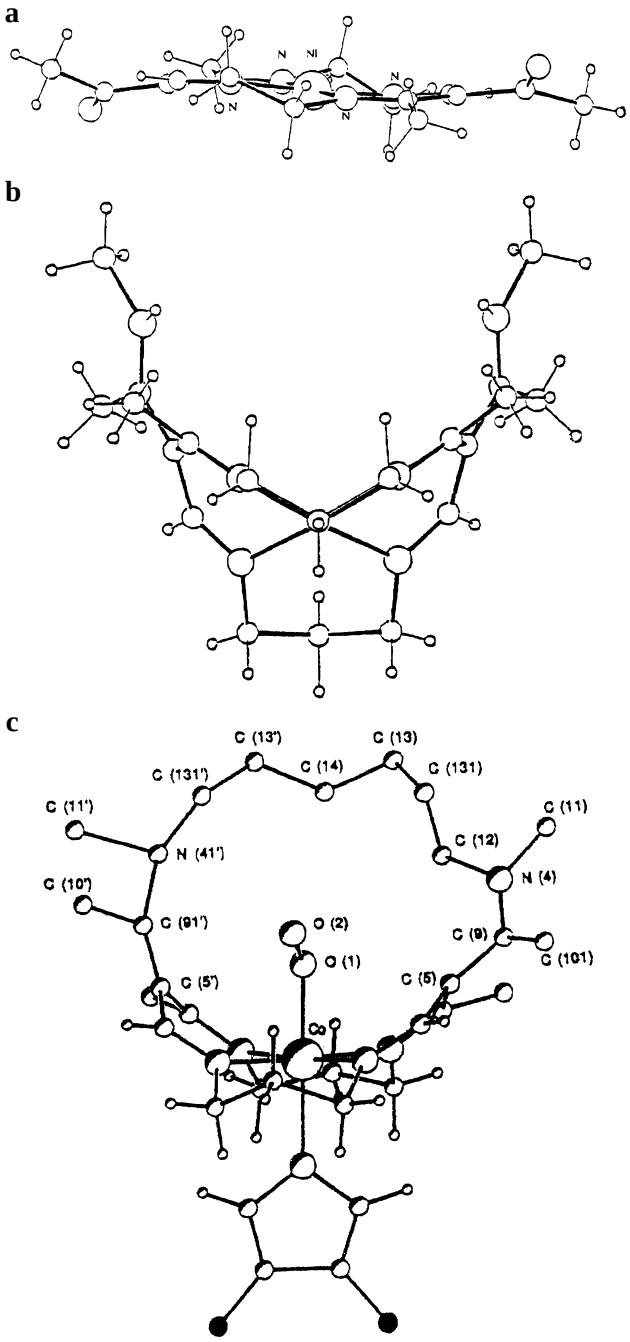

Figure 3. X-ray structures of 14- and 16-membered macrocyclic complexes: (a) Ni(Ac_2HMe[14]Jag): Jäger platform, X = Y = $(CH_2)_2$, $R^1 = R^2 = CH_3$, $R^3 = H$. Reproduced with permission from ref 1. Copyright 1994 American Chemical Society. (b) Cu(H_2MeMe[16]Cyc): unbridged cyclidene, $R^1 = 2Me$, $R^2 = H$, $R^3 = R^4 = Me$, X = Y = $(CH_2)_3$. Reproduced with permission from ref 25. Copyright 1987 American Chemical Society. (c) [Co(C6)MeMe[16]Cyc](MeIm)(O_2): dioxygen adduct with bridged 16-membered cyclidene, $R^1 = (CH_2)_6$, $R^2 = R^3 = R^4 = Me$, X = Y = $(CH_2)_3$. Reproduced with permission from ref 1. Copyright 1994 American Chemical Society.

techniques to study solvation effects in a variety of systems, ranging from simple ions[26] to such biologically important molecules as carbohydrates[27−29] and peptides.[30−32] Computer simulations are becoming increasingly popular in studying host−guest interactions.[33−42] The studies of three-dimensional anisotropic solvent structure have, however, been limited to relatively simple systems, such as pure liquids,[43−45] anthracene in nonpolar (cyclohexane) and polar (2-propanol) solvents,[46] and carbohydrates in water.[27−29] We report here the results of MD simulations of Co([14]Cyc)(MeIm), Co([16]Cyc)(MeIm), and Co(C6[16]Cyc)(MeIm) (Figure 2) in methanol. These macrocyclic (equatorial) ligands were chosen because of their various shapes within metal complexes, as described above. A single axial 1-methylimidazole (MeIm) molecule chemically bound to the cobalt(II) center served two purposes: (1) this axial base is commonly used in the design of dioxygen cariers or redox reagents, to activate the central metal ion; (2) the coordinated MeIm molecule blocks the fifth Co(II) coordination site from the possibility of solvent binding, and this permits unambiguous analysis of the solvation at the sixth (vacant) cobalt(II) coordination site. Methanol was selected as a solvent because (1) the available experimental data on the kinetics of oxygen binding were obtained in this solvent[13,14] and they suggest the absence of solvent molecule binding at the sixth cobalt(II) coordination site; and (2) methanol is a commonly used polar organic solvent, and it also contains hydrophilic OH groups; we believe that the results obtained for methanol solutions will be transferable, to some extent, to both aqueous and nonaqueous solutions.

Methods

Computational Methods. The CHARMM (versions 22 and 24) software package was used for molecular mechanics and molecular dynamics simulations.[47] An all-hydrogen CHARMM force field[48,49] was complemented with the parameters for the macrocyclic framework. Several new atom types were introduced in CHARMM, and the details of the force field parametrization for these atoms (based upon a

(26) Brooks, C. L., III. *J. Phys. Chem.* **1986**, *90*, 6680−6684.
(27) Liu, Q.; Brady, J. W. *J. Am. Chem. Soc.* **1996**, *118*, 12276−12286.
(28) Liu, Q.; Schmidt, R. K.; Teo, B.; Karplus, P. A.; Brady, J. W. *J. Am. Chem. Soc.* **1997**, *119*, 7851−7862.
(29) Schmidt, R. K.; Karplus, M.; Brady, J. W. *J. Am. Chem. Soc.* **1996**, *118*, 541−546.
(30) Van Buuren, A. R.; Berendsen, H. J. C. *Biopolymers* **1993**, *33*, 1159−1166.
(31) Smith, P. E.; Dang, L. X.; Pettitt, B. M. *J. Am. Chem. Soc.* **1991**, *113*, 67−73.
(32) Schiffer, C. A.; Dötsch, V.; Wüthrich, K.; van Gunsteren, W. F. *Biochemistry* **1995**, *34*, 15057−15067.
(33) *Spectroscopic and computational studies of supramolecular systems*; Davies, J. E. D., Ed.; Kluwer: Dordrecht, 1992.
(34) van Veggel, F. C. J. M.; van Duynhoven, J. P. M.; Harkema, S.; Wolbers, M. P. O.; Reinhoudt, D. N. *J. Chem. Soc., Perkin Trans. 2* **1996**, 449−454.
(35) van Helden, S. P.; van Eijck, B. P.; Janssen, L. H. M. *J. Biomol. Struct. Dyn.* **1992**, *9*, 1269−1283.
(36) Koehler, J. E. H.; Saenger, W.; van Gunsteren, W. F. *J. Biomol. Struct. Dyn.* **1988**, *6*, 181−198.
(37) Koehler, J. E. H.; Saenger, W.; van Gunsteren, W. F. *J. Mol. Biol.* **1988**, *203*, 241−250.
(38) Dang, L. X.; Kollman, P. A. *J. Phys. Chem.* **1995**, *99*, 55−58.
(39) Lybrand, T. P.; McCammon, J. A.; Wipff, G. *Proc. Natl. Acad. Sci. U.S.A.* **1986**, *83*, 833−835.
(40) Abidi, R.; Baker, M. V.; Harrowfield, J. M.; Ho, D. S.-C.; Richmond, W. R.; Skelton, B. W.; White, A. H.; Varnek, A.; Wippf, G. *Inorg. Chim. Acta* **1996**, *246*, 275−286.
(41) Fraternali, F.; Wipff, G. *J. Inclusion Phenom. Mol. Recognit.* **1997**, *28*, 63−78.
(42) Papoyan, G.; Gu, K.-J.; Wiorkiewicz-Kuczera, J.; Kuczera, K.; Bowman-James, K. *J. Am. Chem. Soc.* **1996**, *118*, 1354−1364.
(43) Kusalik, P. G.; Svishchev, I. M. *Science* **1994**, *265*, 1219−1221.
(44) Svishchev, I. M.; Kusalik, P. G. *J. Chem. Phys.* **1993**, *99*, 3049−3058.
(45) Svishchev, I. M.; Kusalik, P. G. *J. Chem. Phys.* **1994**, *100*, 5165−5171.
(46) Jas, G. S.; Wang, Y.; Pauls, S. W.; Johnson, C. K.; Kuczera, K. *J. Chem. Phys.* **1997**, *107*, 8800−8812.
(47) Brooks, B. R.; Bruccoleri, R. E.; Olafson, B. D.; States, D. J.; Swaminathan, S.; Karplus, M. *J. Comput. Chem.* **1983**, *4*, 187.
(48) MacKerrel, A. D., Jr.; Wiorkiewicz-Kuczera, J.; Karplus, M. *J. Am. Chem. Soc.* **1995**, *117*, 11946.

vibrational frequency fitting procedure) are provided in ref 50. Atomic charges were obtained from ZINDO calculations[51−53] (single-point energy; Mulliken population analysis), as implemented in the CAChe package (Oxford Molecular Group). These charges appear to be compatible with the force field for the cyclidene macrocycles, allowing us to reproduce a variety of cyclidene geometries observed experimentally.[1,50] Complete topology and parameter listings, including atom types and atomic charges, are summarized in the Supporting Information, Tables 1 and 2; the atom-numbering scheme is shown in Figure 2c (macrocyclic framework, heavy atoms) and the Supporting Information, Figure 1 (all atoms). Standard CHARMM force field parameters and atomic charges[48,49] developed for serine and threonine side chains were used to model the potential energy function for the solvent (methanol) molecules. These parameters provide a model of liquid methanol in excellent agreement with experimental observations (calculated density of 0.79 g/cm^3 and $\Delta H_{vap} = 35.4$ kJ/mol).[54]

Molecular dynamics simulations for Co([14]Cyc), Co([16]Cyc), and Co(C6[16]Cyc) were performed both in a vacuum and in methanol solutions, yielding 200 ps trajectories. PF_6^- anions were not included in the simulation, because they are not coordinated to the central cobalt(II) ions.[1,12] Consequently, no significant influence of the PF_6^- anions on the short-range solvation was expected.[42,55] Possible long-range effects were not subjects of the reported research. The simulation protocol was identical for all systems (except for special features applicable to molecular ensembles, discussed below). For the liquid systems, the simulation conditions corresponded to the isothermal−isobaric ensemble (with the internal pressure set to 1 atm, and the temperature of 300 K), using Langevin dynamics on a pressure piston degree of freedom,[56] and the Nose−Hoover algorithm[57,58] to control the temperature. A truncated octahedral cell[59,60] with periodic boundary conditions was used in all simulations of solvent-containing systems. In molecular dynamics simulations, SHAKE constraints[61] were imposed on bonds involving hydrogen atoms, providing a 2 fs time step.[62] The equations of motion were integrated by using a Verlet algorithm.[63] In energy calculations, a 12.0 Å nonbonded cutoff distance was employed, with a switching function between 10.0 and 12.0 Å for van der Waals terms and a shift function at 12.0 Å for electrostatic terms, in order to eliminate discontinuities due to the cutoff.[47]

The same simulation protocol was used for all three macrocycles in methanol solutions. The initial geometry of Co([16]Cyc) was taken from the X-ray structure of the analogous copper complex;[25] the initial geometry for Co(C6[16]Cyc) was taken from X-ray data.[1,64] Methylimidazole was positioned, as in [Co(C6[16]Cyc)(O_2)(MeIm)] (X-ray data[12]). Energy minimization for both compounds yielded structures very close to the initial X-ray geometries (in support of adequacy of the force field developed for cyclidene complexes[50]). For the case of Co[14]Cyc, the saddle-shaped conformation of Co([16]Cyc), with two carbon atoms deleted (and bond, angle, and dihedral energy terms modified accordingly), was used as the initial structure. In complete agreement with the experimental X-ray data for 14-membered cyclidenes,[25,65] the "flat" (open) conformation was obtained after energy minimization. For all three macrocycles, the optimized molecule was placed in the center of a preequilibrated methanol cell (based on a cube of ca. 38 Å edge; the exact size of the cell depends on the linear dimensions of the particular macrocycle and was selected in order to ensure that a solvent layer of at least 10 Å surrounds the macrocycle molecule within the primary cell). After deletion of the methanol molecules overlapping the solute, the Co([16]Cyc), Co(C6[16]Cyc), and Co([14]Cyc) systems contained 393, 392, and 433 methanol molecules, respectively. After brief energy minimization, heating, and 10 ps constant volume equilibration, the systems were allowed to evolve at constant pressure for 20 ps each, followed by 200 ps production runs (at constant pressure of 1 atm). Coordinate sets were saved every 0.2 ps for subsequent analysis. The average temperature for all three systems was 300 ± 5 K, and the average box size was 38.25 ± 0.16, 38.26 ± 0.17, and 39.37 ± 0.15 Å for Co([16]Cyc), Co(C6[16]Cyc), and Co([14]Cyc), respectively.

In order to compute the three-dimensional anisotropic solvent distribution around the macrocycle molecule, the procedure developed and applied to the studies of anthracene solvation[46] was adopted. The whole system was oriented to the principal axis system of selected atoms of the solute. The in-plane cobalt(II) coordination sphere (four nitrogen atoms in the macrocyclic ring) is rigid in our systems, and the solvent distribution about the cobalt(II) center is of primary interest. For these reasons, four donor nitrogen atoms, along with four adjacent carbon atoms from the saturated chelate rings, were selected. In this case, the cobalt(II) ion lies practically at the center of mass of the eight-atom system, and the $Co(N_4)$ plane coincides with the *xy* plane (with the principal axes *x* and *y* bisecting the Co−N bonds). The oriented system (including the primary cell and the images) was partitioned into small cubes with sides of 0.5 Å, and the methanol center-of-mass distribution was computed by direct count and then averaged over the trajectory. Two-dimensional slices of the 3D solvent distribution were analyzed, using contour plots. Similar procedures have been applied previously to a variety of systems, ranging from pure liquids,[43−45] to carbohydrates in water,[27−29] to crystalline hydrated proteins.[66] Brady and co-workers[28] pointed out that system reorientation at every trajectory frame leads to inadequate statistics in the corners of the cube. Reliable statistics are obtained in a sphere with a radius equal to a minimal distance from the origin to the edge of the primary cell. In the case of the truncated octahedral cell based on a cube of side a, this radius is equal to $a(\sqrt{3})/4 = 0.43a$. This should be taken into account in analyzing the anisotropic solvent structure (see discussion accompanying Figures 10 and 11).

Experimental Methods. The solvents and reagents used in these studies were of reagent grade or better. *N*-Methylimidazole was dried over barium oxide and distilled in vacuo; acetonitrile was dried over calcium hydride and distilled. The solvents were degassed by successive freeze−pump−thaw cycles prior to use. The syntheses and manipulation of the cobalt(II) complexes were performed under an atmosphere of dry, oxygen-free nitrogen in a Vacuum Atmospheres glovebox, with the oxygen content below 5 ppm. Co([16]Cyc)(PF_6)$_2$ was synthesized by analogy to a published procedure.[12,64,67] Dioxygen affinities were determined by spectrophotometric titration with dioxygen[12,64] carried out in a 1 cm gastight quartz cell with a bubbling tube. Spectra were recorded on a Varian 2300 spectrometer connected via an IEEE interface to an IBM PC which provided automatic instrument control and data

(49) MacKerrel, A. D., Jr.; Bashford, D.; Bellott, M.; Dunbrack, R. L., Jr.; Evanseck, J. D.; Field, M. J.; Fischer, S.; Gao, J.; Guo, H.; Ha, S.; Joseph-McCarthy, D.; Kuchnir, L.; Kuczera, K.; Lau, F. T. K.; Mattos, C.; Michnik, S.; Ngo, T.; Nguyen, D. T.; Prodhom, B.; Reiher, W. E., III; Roux, B.; Schlenkrich, M.; Smith, J. C.; Stote, R.; Straub, J.; Watanabe, M.; Wiorkiewicz-Kuczera, J.; Yin, D.; Karplus, M. *J. Phys. Chem. B* **1998**, *102*, 3586−3616.
(50) Rybak-Akimova, E. V.; Kuczera, K. *Inorg. Chem.*, manuscript in preparation.
(51) Ridley, J. E.; Zerner, M. C. *Theor. Chim. Acta* **1976**, *42*, 223.
(52) Bacon, A. D.; Zerner, M. C. *Theor. Chim. Acta* **1979**, *53*, 21.
(53) Zerner, M. C.; Loew, G. H.; Kirchner, R. F.; Mueller-Westerhoff, U. T. *J. Am. Chem. Soc.* **1980**, *102*, 589.
(54) Jas, G. S.; Kuczera, K. Unpublished results.
(55) Wiorkiewicz-Kuczera, J.; Bowman-James, K. In *Supramolecular Chemistry of Anions*; Bianchi, A., Bowman-James, K., Garcia-Espana, E., Eds.; Wiley-VCH: New York, 1997; pp 335−354.
(56) Feller, S. E.; Zhang, Y. H.; Pastor, R. W.; Brooks, B. R. *J. Chem. Phys.* **1995**, *103*, 4613−4621.
(57) Nose, S. *J. Chem. Phys.* **1984**, *81*, 511.
(58) Hoover, W. G. *Phys. Rev. A* **1985**, *31*, 1695.
(59) Adams, D. J. *Chem. Phys. Lett.* **1979**, *62*, 329.
(60) This function gives the probability of finding a pair of atoms at a distance *r* apart, relative to the probability expected for a completely random distribution at the same density. Allen, M. P.; Tildesley, D. J. *Computer Simulations of Liquids*; Clarendon: Oxford, 1987.
(61) Ryckaert, J. P.; Ciccotti, G.; Berendsen, H. J. C. *J. Comput. Phys.* **1977**, *23*, 327.
(62) Barth, E.; Kuczera, K.; Leimkuhler, B.; Skeel, R. D. *J. Comput. Chem.* **1995**, *16*, 1192.
(63) Verlet, L. *Phys. Rev.* **1967**, *159*, 98−103.
(64) Stevens, J. C.; Jackson, P. J.; Schammel, W. P.; Christoph, G. G.; Busch, D. H. *J. Am. Chem. Soc.* **1980**, *102*, 3283.
(65) Chen, J.; Ye, N.; Alcock, N. W.; Busch, D. H. *Inorg. Chem.* **1993**, *32*, 904−910.
(66) Thanki, N.; Thornton, J. M.; Goodfellow, J. M. *J. Mol. Biol.* **1988**, *202*, 637−657.
(67) Cairns, C. J.; Busch, D. H. *Inorg. Synth.* **1990**, *27*, 261.

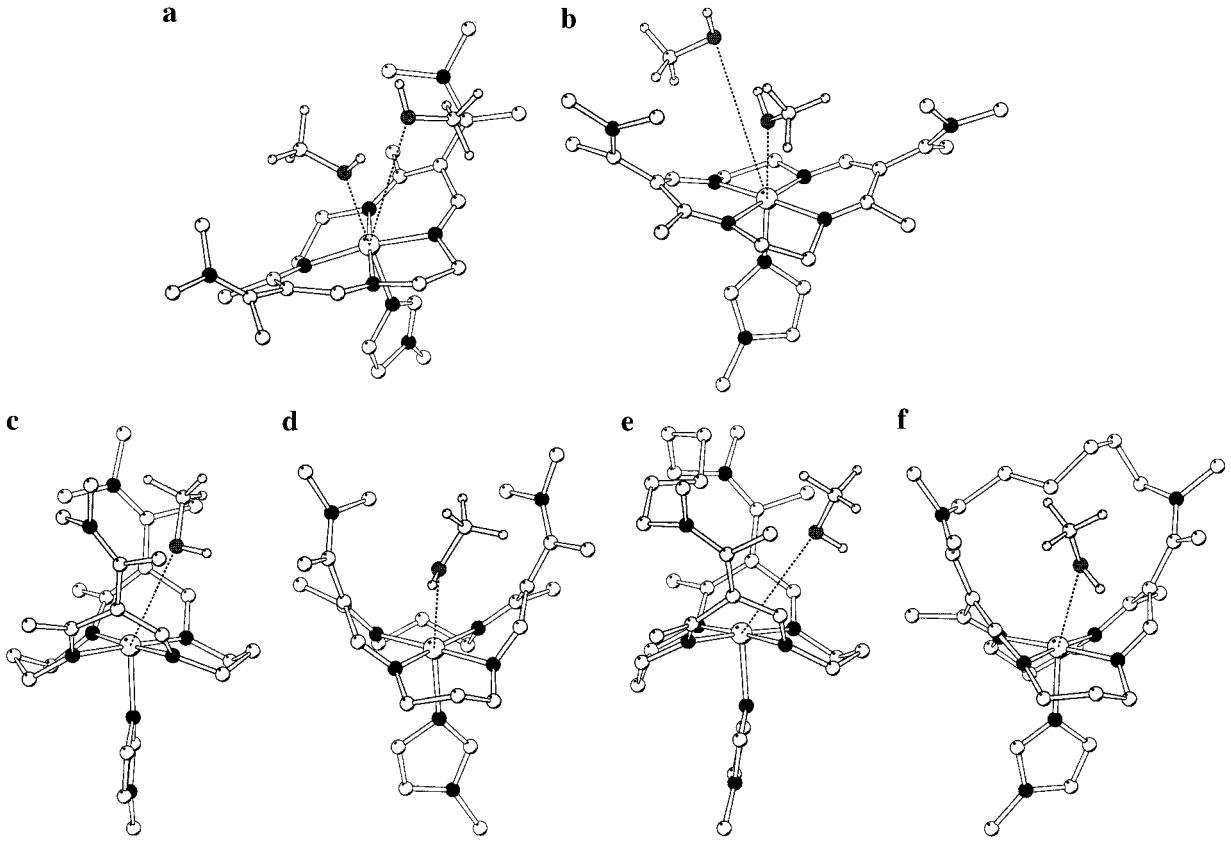

Figure 4. Trajectory snapshots from simulations in methanol: (a,b) Co([14]Cyc); (c,d) Co([16]Cyc); (e,f) Co(C6[16]Cyc). Methanol molecules within 5 Å from the Co(II) center are shown.

collection. Dioxygen/nitrogen gas mixtures were generated using Tylan FC-260 mass flow controllers.

Results and Discussion

The main objective for this research is to compare solvation of the three systems, which are very similar electronically, but substantially different in their preferential conformations. In the following sections, the results of molecular dynamics simulations on solvated macrocyclic complexes are analyzed in terms of macrocycle structure and dynamics, and solvent structure and dynamics. Experimental data on dioxygen affinities for 16-membered cobalt(II) cyclidenes will be presented last and interpreted in view of the simulation results.

Qualitative System Characterization Based on Molecular Graphics. The time evolution of the distances between "terminal" carbon atoms at the "edges" of the macrocycle (C3−C19, d1), exocyclic carbon atoms (C39−C40, d2), and the exocyclic nitrogen atoms (N45−N58, d3) (Figure 2c) shows that the complexes undergo no significant conformational changes throughout our 200 ps simulations. The 14-membered macrocycle remains essentially planar during the course of the simulation; the 16-membered unbridged complex retains its saddle shape, and both the macrocyclic framework and the hexamethylene bridge preserve their conformations in the case of the C6-bridged cyclidene derivative. For a given macrocycle, there is no qualitative difference in ligand structure between vacuum and solvent simulations; quantitative difference will be discussed below. However, the simulations in methanol reveal distinct qualitative differences in the solvation of the three complexes. Snapshots of the trajectories for three complexes in methanol are shown in Figure 4.

For [14]Cyc we find one strongly bound methanol molecule directly above the cobalt ion, with a Co···O(MeOH) distance of ca. 2.5 Å. One measure of the strength of this direct electrostatic interaction is that the same methanol (MeOH) molecule remains bound at this site throught the 200 ps simulation (see below for a more quantitative measure). Because of the relatively open structure of the 14-membered-ring derivative, one or two more MeOH molecules can reside above the cyclidene plane with Co···O distances below 5.0 Å.

In the unbridged [16]Cyc system a specifically bound MeOH molecule is also seen close to the Co atom. Due to the saddle shape of the cyclidene ring, this methanol cannot approach the Co ion directly from above, but does so preferentially from the less crowded side of the ring, opposite the methyl substituents and amino groups. This MeOH molecule resides at typical Co···O distances of 3.0−4.0 Å. As in the [14]Cyc system, the same methanol occupies the binding site throughout the 200 ps simulation.

In the bridged [16]Cyc system a methanol molecule may be found in a position similar to that found in the "unbridged" simulation, but further away from the Co, with typical Co···O distances between 3.5 and 5.0 Å. This molecule is quite labile; three different methanols occupy this site at different points in time, during the 200 ps MD simulation, indicating that the Co···MeOH interactions are weaker than those in the unbridged [14]Cyc and [16]Cyc cases. For both the bridged and unbridged 16-membered macrocycles no other methanols, except for those specifically bound, appear within a Co···O distance of 5.0 Å.

It should be noted that all methanol molecules are initially equivalent in our systems, and none of them is chemically bound to the cobalt atom (that is, no explicit Co−O bond was introduced in the topology file). The preferential location of methanol molecules at a short distance from the cobalt(II) for unbridged complexes is exclusively due to nonbonding interactions.

Table 1. Trajectory-Averaged Cavity Width for Three Cobalt Complexes, Compared to Crystal Geometry

	distance, Å (rms fluctuations)		
structural parameter	Co([14]Cyc)	Co([16]Cyc)	Co(C6[16]Cyc)
d1 (C3−C19)			
dynamics in a vacuum	6.37 (0.15)	5.14 (0.18)	5.47 (0.15)
dynamics in methanol	6.35 (0.12)	5.06 (0.15)	5.31 (0.17)
X-ray data (cryst)		5.28[b]	5.29[c]
d2 (C39−C40)			
dynamics in a vacuum	8.89 (0.29)	6.29 (0.35)	6.94 (0.28)
dynamics in methanol	8.84 (0.22)	6.16 (0.25)	6.63 (0.31)
X-ray data (cryst)	9.73[a]	6.49[b]	6.63[c]
d3 (N45−N58)			
dynamics in a vacuum	9.61 (0.55)	6.05 (0.38)	7.09 (0.23)
dynamics in methanol	9.56 (0.38)	5.94 (0.33)	6.85 (0.27)
X-ray data (cryst)	10.67[a]	6.39[b]	6.74[c]

[a] X-ray data are available for the bridged complex Ni(C12)-MeMe[14]Cyc, X = Y = $(CH_2)_2$, $R^1 = (CH_2)_{12}$, $R^2 = R^3 = R^4$ = Me (Figure 2), ref 65. [b] Cu(H_2MeMe[16]Cyc), X = Y = $(CH_2)_2$, R^1 = 2Me, R^2 = H, $R^3 = R^4$ = Me (Figure 2), ref 25. [c] Co(C6MeMe[16]Cyc), X = Y = $(CH_2)_3$, $R^1 = (CH_2)_6$, $R^2 = R^3 = R^4$ = Me (Figure 2), refs 1, 12.

Hydrogen atoms of the methanol molecules within the first solvation sphere are not hydrogen-bonded to any of the macrocyclic nitrogen atoms.

Geometry of the Macrocycles in a Vacuum and in Methanol Solutions. Earlier studies have shown that the dioxygen affinity of the cobalt(II) complexes of the 16-membered bridged cyclidenes correlates with the cavity width of the macrocycle, with the width defined as the distance between N45 and N58 atoms (Figure 2c).[1,12] The cavity widths determined by X-ray crystallography, obviously, refer to the molecular geometry in the solid state. Molecular mechanics calculations for isolated cyclidene molecules in the gas phase (using either previously developed MM2/MMP2 force field[68] and our extended CHARMM force field[50]) reproduce the crystallographic cavity width fairly well.[50,65,68] The atomic fluctuations in cyclidene molecules may, however, change the time-averaged cavity width, compared to the cavity width in the optimized structures. Solvation is also expected to alter the macrocyclic geometry to some extent. Time evolution of macrocycle conformations, both in a vacuum and in methanol solutions, has been deduced from our simulations.

For all systems studied, no significant conformational changes in the macrocycle occurred during 200 ps simulations. The trajectory-averaged macrocyclic geometry for each complex, obtained in vacuum simulations, proved to be very similar to the corresponding optimized structures obtained from molecular mechanics calculations. The geometric parameters related to the cavity size are summarized in Table 1, along with available X-ray data for similar compounds.[1,25,64,65] Crystallographic information for 14-membered cyclidenes is limited to the unbridged Jäger precursor which has carbonyl groups in place of dimethylamino groups, and to the C12-bridged [14]cyclidene complex. Thus, a ca. 1 Å discrepancy in the cavity width of the unbridged 14-membered complex between that obtained in MD simulations and the cavity width of the C12-bridged complex determined crystallographically (Table 1) is not surprising.

In the case of "open" Co([14]Cyc), the label "cavity width" is a misnomer, since the structure is flat and has no cleft. In this case the average "cavity width" is actually, just the distance between selected pairs of carbon or nitrogen atoms, and it is practically identical in a vacuum and in methanol. Thus, the "flat" conformation of the 14-membered macrocycle is insensitive to solvent. The root-mean-square (rms) fluctuations in the distance between the macrocyclic carbon atoms C3 and C19 are significantly smaller than the rms fluctuations in the distances between exocyclic carbon (C39 and C40) or nitrogen (N45 and N58) atoms, indicating the relative rigidity of the macrocyclic framework. The rms fluctuations of the exocyclic atoms are greater for vacuum simulations than for solution simulations.

The unbridged Co([16]Cyc), unlike its 14-membered counterpart, does have a well-defined cavity, which is much smaller than the so-called "cavity width" for Co([14]Cyc) (Table 1). The time-averaged cavity width does not differ substantially for the molecule in a vacuum and the molecule in methanol solution, being only slightly smaller in the latter case. The rms fluctuations in interatomic distances are again higher for vacuum simulation, as compared to the simulation in the solvent. The exocyclic atoms are more flexible than the atoms within the macrocycle, as is reflected in higher rms fluctuations in d2 and d3, as compared to d1.

The behavior of the bridged complex Co(C6[16]Cyc) differs from the behavior of both unbridged complexes (Co([14]Cyc) and Co([16]Cyc)). The trajectory-averaged cavity width of this bridged complex in methanol solution is noticeably smaller than its cavity width in a vacuum (by 0.16 Å in d1; 0.31 Å in d2; and 0.24 Å in d3). The rms fluctuations in d1, d2, and d3 do not change upon transition from vacuum to methanol. The exocyclic carbon and nitrogen atoms are still somewhat more flexible than the atoms within the macrocycle, but the difference is smaller in comparison with the unbridged complexes.

It can be concluded that, among the three systems studied, only the structure of bridged Co(C6[16]Cyc) is substantially affected by solvation, while the structures of unbridged compounds are essentially uninfluenced by the solvent. This result is somewhat counterintuitive. One might expect that more rigid bridged compound would be less sensitive to the environment than its more flexible unbridged analogues. The most probable cause for the observed behavior is the exclusion of solvent from the cavity, resulting in a solvation mode for the bridged complex that is directed solely from *outside the cavity*. This solvation mode can "compress" the molecule, leading to the observed decrease in the cavity width. In the case of flat 14-membered cyclidene, there is no cavity and solvent molecules are present both above and below the plane that approximates the locations of most of the atoms in the structure. This completely "open" conformation is not altered upon solvation. In the intermediate case of unbridged saddle-shaped Co([16]Cyc), the methanol molecules tend to enter the cavity, thus "pushing apart" the cavity walls. This balances the effect of the "outside-the-cavity" solvation.

The substantial differences in molecular shapes of crystalline complexes with [14]Cyc, [16]Cyc, and C6[16]Cyc are preserved in the course of molecular dynamics in solvent. Consequently, the results of these 200 ps simulations can be used for comparison of solvation of differently shaped molecules.

Analysis of Three-Dimensional Solvent Structure in Macrocyclic Complex−Methanol Systems. (a) Isotropic Solvent Distribution. The radial distribution of the solvent molecules around the cobalt central atom has been analyzed in terms of time evolution of the minimum Co−O(MeOH) distance (the distance from the cobalt atom to the nearest methanol oxygen atom) and trajectory-averaged pair distribution functions. The presence of covalently bound methylimidazole as an axial ligand

(68) Lin, W.-K.; Alcock, N. W.; Busch, D. H. *J. Am. Chem. Soc.* **1991**, *113*, 7603−7608.

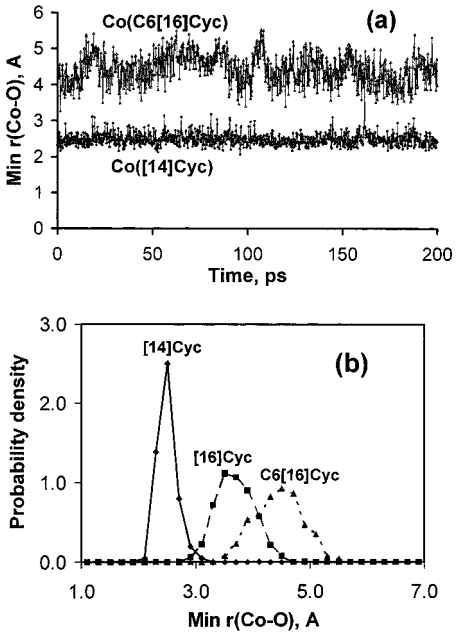

Figure 5. (a) Time evolution of the minimum Co−O(MeOH) distance in the course of 200 ps simulations for Co([14]Cyc) and Co(C6[16]-Cyc) in methanol. (b) Probability distribution of the minimum Co−O(MeOH) distance for the three complexes studied.

in all systems effectively screens the cobalt atom from the solvent molecules approaching it from one side of the macrocycle. Consequently, it is expected that the radial distribution of the solvent, at least at short Co−O(MeOH) distances, reflects the solvent distribution inside the "cleft" of the cyclidene complexes. The analysis of anisotropic solvent structure around the macrocycles discussed below confirms this hypothesis.

The distance between the cobalt atom and the oxygen atom in the methanol molecule closest to cobalt(II), for Co([14Cyc]), Co([16Cyc]), and Co(C6[16]Cyc), is shown in Figure 5. This solvent molecule is located at a significantly shorter Co−O distance in the case of the planar complex (ca. 2.5 Å) than it is in the saddle-shaped unbridged complex (ca. 3.7 Å). The solvent is pushed even farther away (to ca. 4.5 Å) in the lacunar C6-bridged complex. The rms fluctuations in Co−O(MeOH) distance are small for Co([14]Cyc) (0.2 Å), where the solvent is located close to the cobalt(II) atom and appears to be relatively tightly bound (see also discussion below). The amplitude of methanol fluctuations increases substantially with an increase in the Co−O(MeOH) distance, as can be seen for Co([16]Cyc) (0.3 Å) and Co(C6[16]Cyc) (0.4 Å), reflecting weaker interactions.

The pair distribution functions for the Co atom within the macrocycle and the oxygen atoms of the methanol molecules[60] are distinctly different for the three complexes (Figure 6) and reflect the structural properties of the solvated complexes. This difference is also reflected in the number of methanol molecules around the cobalt center calculated as an integral of $g(r)$ (Figure 7). The data indicate the presence of one well-localized, strongly bound methanol molecule at a distance of 2.5 Å from Co([14]-Cyc), a more weakly bound methanol at a distance of 3.7 Å from Co([16]Cyc), and a still more labile and longer-range complex for the bridged species Co(C6[16]Cyc).

In terms of the structure, the increase in $g(r)$ at Co−O distances greater than 5 Å is due to the presence of methanol molecules approaching from the side of the cyclidene ligand on which imidazole is bound to cobalt. At any given Co−O(MeOH) distance, the number of methanol molecules within this shell decreases in the order Co([14]Cyc) > Co([16]Cyc) > Co(C6[16]Cyc).

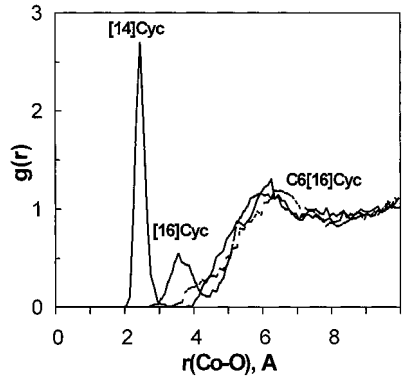

Figure 6. Radial pair distribution function for methanol oxygen atoms around the central Co atom calculated from the MD simulations for three macrocyclic complexes.

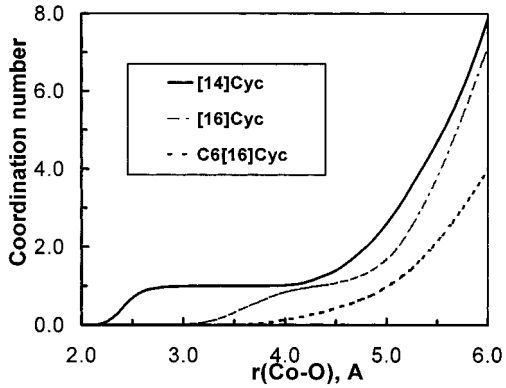

Figure 7. Trajectory-averaged number of methanol oxygen atoms ("coordination number") within a sphere of a given radius around the central Co atom, calculated as an integral of the pair distribution function. Statistical fluctuations in $N(r)$, determined by dividing the trajectory points into five consecutive subsets and evaluating the standard deviation of the mean of the block subaverages, are ca. 10%.

To estimate the strength of the Co−O interactions in the different cyclidene derivatives we can convert the pair distribution functions $g(r)$ to potentials of mean force $G(r)$:[69]

$$G(r) = -kT \ln g(r) \qquad (1)$$

An interpretation of free energy profiles calculated with eq 1 requires caution, because the sampling of high-energy regions in the standard simulations is not adequate. The results (Figure 8) are still meaningful, however, for the purpose of comparison of three closely related, yet structurally different, systems. For the [14]Cyc system the $G(r)$ profile has a minimum at −0.7 kcal/mol at 2.4 Å. The negative value of $G(r)$ indicates that the specifically bound methanol interacts with the Co^{2+} ion more strongly than a typical MeOH molecule interacts with its neighbors in bulk solvent. The 0.7 kcal/mol represents the reversible work needed to move a methanol molecule from the specific cobalt binding site at 2.4 Å to bulk solvent (where $g = 1$ and $G = 0$). A free energy barrier of at least 4 kcal/mol separates the flat profile characteristic of bulk solvent obtained for $r > 6.5$ Å from the free energy minimum. This barrier cannot be estimated more precisely from our simulations, since we found no occurrences of Co−O distances in the 3.8−4.0 Å range. The existence of this barrier indicates that favorable

(69) Beveridge, D. L.; DiCapua, F. M. *Annu. Rev. Biophys. Biophys. Chem.* **1989**, *18*, 431−492.

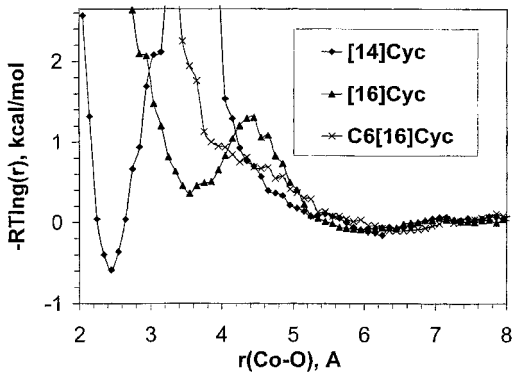

Figure 8. Potential of mean force, calculated as $-RT \ln (r) +$ constant, for methanol oxygen atoms around the central cobalt atom in three macrocyclic complexes. The absence of data points (line breaks) reflects the absence of oxygen atoms at a given distance from the cobalt atom in the simulations ($g(r) = 0$) because of the insufficient sampling in high-energy regions, and formally corresponds to infinite positive free energy (infinitely high barriers).

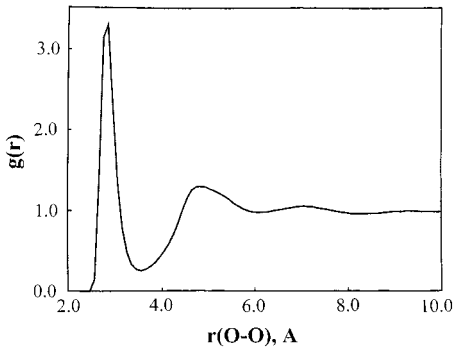

Figure 9. Radial pair distribution function for solvent methanol oxygen atoms $g_{OO}(r)$ for Co([16]Cyc).

interactions with other solvent molecules are broken when the strongly bound MeOH occupies its binding site. A second minimum in $G(r)$ is seen close to 6.0 Å; it is relatively broad and shallow and corresponds to the broad peak in $g(r)$ representing the first full solvation shell of the cyclidene.

For the saddle-shaped unbridged [16]Cyc, $G(r)$ has a minimum of 0.4 kcal/mol at 3.5 Å.

The positive value of $G(r)$ indicates that methanol interactions are stronger in bulk solvent than at the specific binding site. This minimum is separated by a ca. 1 kcal/mol barrier from the rest of the relatively flat profile. Again, this barrier represents the breaking of favorable MeOH···MeOH interactions in the formation of the specific complex. Finally, for the bridged C6-[16]Cyc system, the $G(r)$ presents an essentially featureless, monotonically decreasing profile, in accord with the shape of the pair distribution function $g(r)$.

The structure of the bulk solvent in our simulations, exemplified by the self-distribution function $g(r)$ for O(MeOH)−O(MeOH) pairs (Figure 9), is typical of hydrogen-bonded liquid alcohols.[45,70]

(b) Anisotropic Solvent Structure. It can be concluded from the above discussion that the radial solvent distribution about the cobalt(II) ion in the cyclidene complexes is clearly different for the three differently shaped compounds. Analysis of the three-dimensional solvent structure in these systems helps us understand details of the solvation pattern characteristic of each system. In particular, the solvent distribution within the cleft or lacuna of the macrocycle, located in the position that is trans to the axially coordinated 1-methylimidazole, is of primary interest. The trajectory-averaged solvent density about each of the macrocycles has been computed as a normalized number of counts of the center of mass of methanol molecules in 0.5 Å cubic bins. Two-dimensional slices of the solvent density in *xy*, *yz*, and *xz* planes are shown, as contour plots, in Figure 10.[71] In all cases, the cobalt(II) atom lies in the origin. The $z = 0$ plane (*xy* plane) coincides with the CoN_4 plane of the macrocyclic complexes, and the *y* axis is directed toward the unsaturated chelate ring, while the *x* axis goes through the saturated chelate rings. For each of the macrocycles, the contour of the molecule in the *xy* plane is well-defined and free of solvent. The *x* dimensions of all three complexes are comparable, which is expected because of the similarity of the structures of their saturated chelate rings. The solvent molecules found in the *xy* solvation shell, however, are still far from the cobalt(II) center (at a distance of 5 Å or greater) and are separated from the cobalt atom by the macrocyclic ligand. Consequently, these methanol molecules will not directly influence reactions at the sixth coordination site of the cobalt(II).

Figure 10 also shows cross sections of the cavities for each of the complexes in *yz* and *xz* slices. It is clear that no solvent molecules are located within the lacuna of the bridged complex Co(C6[16]Cyc). In the case of the saddle-shaped unbridged complex Co([16]Cyc), no methanol molecules are located above the cobalt(II) center; some solvent density can be seen, however, at the openings into the cavity. Methanol molecules can enter the cleft, but they do not occupy the inner part of the cleft. These molecules will, to some extent, affect the reactions at the cobalt(II) coordination site, because they will interfere with sixth-ligand binding. This influence is not, however, as significant as can be predicted for the planar 14-membered complex Co([14]Cyc) (Figure 10). For the latter complex, significant solvent density is found not only on the sides of the cavity but also directly above the metal center, at a short distance of ca. 3 Å.

A more detailed picture of solvent structure within the macrocyclic cavity located above the cobalt(II) center can be seen in Figure 11, where the solvent density is shown for several planes for which $z =$ constant. These planes are parallel to the CoN_4 plane of the macrocycle and are shifted along *z* by 2, 3, 4, 5, 6, and 7 Å, respectively. For the bridged lacunar complex Co(C6[16]Cyc), the solvent-free area above the cobalt(II) center gradually shrinks with an increase in distance from the Co(II) atom, but does not completely disappear even at a distance of 7 Å. No solvent molecules are found directly above the metal ion. The combination of the "walls" and the bridge effectively shields the central metal ion from the solvent. For the saddle-shaped unbridged complex, the pattern is generally similar, but some solvent density is clearly present in the cavity in the 4 and 5 Å slices. It is clear that the solvent enters the cavity from the sides, but does not move to the middle of the cleft. The solvent molecules are not located directly above the metal ion. Thus, the screening of the cobalt(II) center from the solvent is also accomplished in the saddle-shaped unbridged complex, but

(70) Haughney, M.; Ferrario, M.; McDonald, I. R. *J. Phys. Chem.* **1987**, *91*, 4934.

(71) As a consequence of cell reorientation at every trajectory frame, solvent density in the corners of the cell is not a periodic function. This complication is discussed in detail in ref 28. Reliable statistics corresponding to the primary cell hold within a sphere of a radius $a/2$ for a cubic cell (see ref 28), or $a\sqrt{3}/2$ for a truncated octahedral cell (the minimum dimension of a primary cell). In our case, $a \approx 38$ Å, and reliable statistics are obtained for a sphere of radius 16.3 Å. It does not limit the discussion, because long-range features are not the primary focus of this project.

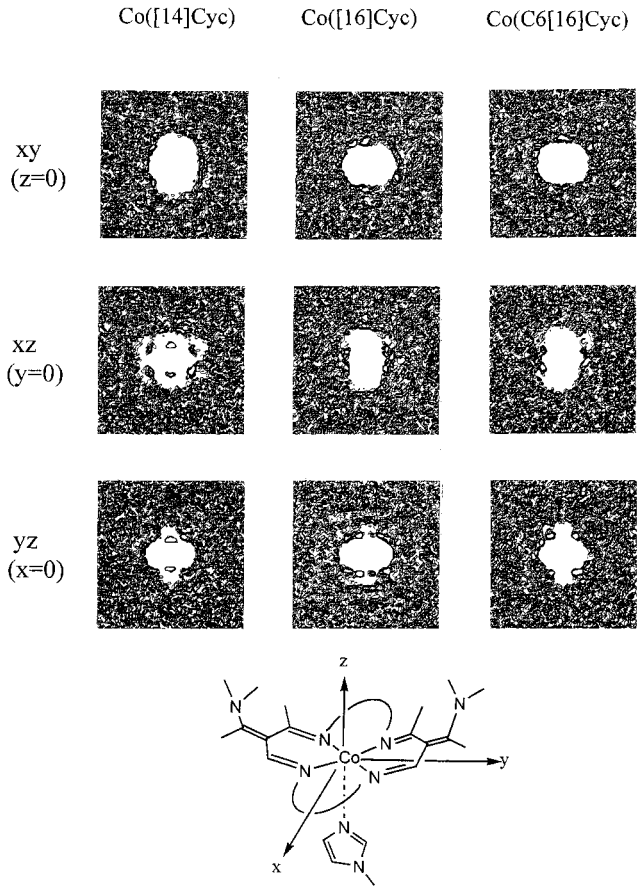

Figure 10. Distribution of methanol molecule centers of mass around the oriented solute (Co([14]Cyc), Co([16]Cyc), and Co(C6[16]Cyc)): *xy*, *xz*, and *yz* slices. The sides of the squares are equal to 36 Å.

this screening is less complete and efficient than in the case of the bridged complex. In the planar 14-membered complex, the metal ion is exposed to the solvent. Significant solvent density is found directly above the metal ion at distances of 3 and 4 Å; the periphery of the macrocycle is also solvated. The solvent-free area completely disappears at 7 Å above the Co atom (in contrast to the behavior of both 16-membered complexes). It can be concluded that the sixth coordination site at the Co(II) ion is extensively solvated in the planar Co([14]Cyc). A similar result has been obtained recently in the simulations of a tetraazamacrocyclic ligand (cyclen) in water: a water molecule was located right above the center of the planar ligand, at a distance of about 3 Å.[72]

No long-range ordering of the solvent, due to the presence of the macrocyclic complexes, has been observed in our systems. This result indicates that methanol−methanol interactions are generally stronger than methanol−solute interactions. Similar behavior has been previously observed for an anthracene−2-propanol system.[46] In contrast, several solvation shells were identified in the anthracene−cyclohexane system,[46] where solvent−solvent interactions are weak. The structure of the extensively hydrogen-bonded solvent (water) can be perturbed by highly hydrophilic solutes, e.g., carbohydrates. At least two distinct solvation shells were seen in simulations of several sugars in water.[27−29]

The qualitative conclusions described above are confirmed by the quantitative determination of the number of methanol molecules within the macrocyclic cleft. For the purpose of comparison between three different systems, a somewhat arbitrary, but uniform, definition of the cleft was used. A square layer of bins surrounding a Co atom (6.5 × 6.5 Å) was selected as the base of the box, and the number of solvent molecules in the layers above this base was counted and averaged over the trajectory. The results on the number of methanol molecules within each layer, as well as the total number of methanol molecules within the box of a given depth, are presented in Table 2 and Figure 12. For the bridged lacunar complex Co(C6[16]Cyc), the 4.25 Å deep box contains only 0.1 solvent molecule, the 4.75 Å deep box includes 0.3 methanol molecule, and a 5.25 Å deep box incorporates 0.4 methanol molecule (the counts were averaged over the trajectories, giving fractional numbers). For the saddle-shaped unbridged compound Co([16]Cyc), an appreciable amount of methanol also appears only in the 4.25 Å deep box, but it grows substantially faster with an increase of box depth, with 0.7 methanol molecule found in a 5.25 Å deep box. In the case of planar complex Co([14]Cyc), a 3.75 Å deep box already has 0.7 methanol molecule in it. The number of methanol molecules slightly exceeds 1 in a 4.25 Å deep box and continues to grow, reaching 1.5 in a 5.25 Å deep box. The difference between inside-the-cleft solvation of the three complexes is illustrated in Figure 12.

The solvent distribution in the cavities of the three complexes, at relatively short distances from the cobalt atom, parallels the radial solvent distribution estimated from the pair distribution function (compare Figures 6 and 12b; Figures 7 and Figure 12a).[73]

Dioxygen Affinity of Co([16]Cyc). Equilibrium constants for dioxygen binding to the title complexes were obtained from oxygen titration experiments. The measurements were conducted

(72) Udomsub, S.; Hannongbua, S. *J. Chem. Soc., Faraday Trans.* **1997**, *93*, 3045−3052.

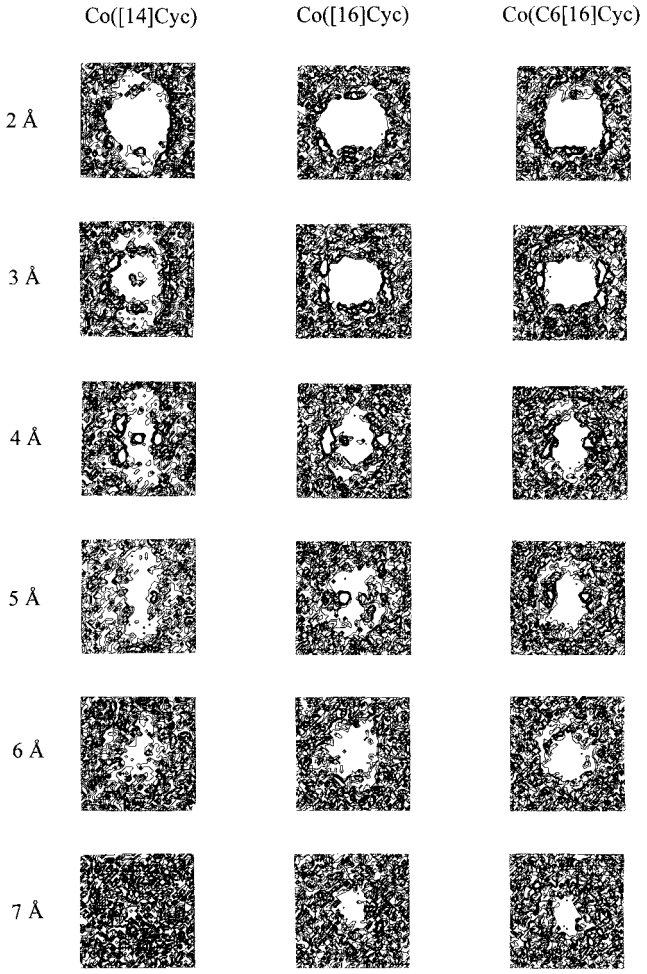

Figure 11. Distribution of methanol molecule centers of mass around the oriented solute: slices parallel to the $Co(N_4)$ plane, crossing the macrocyclic cleft at a different distance from the origin (Co atom) (Z = constant). The sides of the squares are equal to 20 Å.

Table 2. Trajectory-Averaged Number of Methanol Molecules within the Macrocyclic Cavity

	trajectory-averaged no. of methanol molecules[b]		
cavity height, Å[a]	Co([14]Cyc)	Co([16]Cyc)	Co(C6[16]Cyc
3.25	0.032	0.001	0
3.75	0.730	0.008	0.007
4.25	1.067	0.058	0.093
4.75	1.350	0.474	0.298
5.25	1.506	0.721	0.410

[a] The cavity has been defined as a box with a square base having a Co atom in the middle and four nitrogen donor atoms close to the corners, with a side of 6.5 Å. Cavity height corresponds to the box height. [b] The methanol center of mass within the cavity has been counted. The number of methanol molecules within the cavity in individual trajectory frames varies between 0 and 1 for Co(C6[16]Cyc); 0, 1, and (rarely) 2 for Co([16]Cyc); and 0, 1, and 2 for Co([14]Cyc).

in acetonitrile solutions, because thermodynamic parameters for oxygenation of a variety of cyclidene complexes, including Co(C6[16]Cyc), are available for this solvent.[1,12] It has also been shown that dioxygen affinities of cobalt cyclidene complexes, measured in the presence of a strong axial base (such as methylimidazole), are essentially solvent-independent.[1,12] A similar result, insensitivity to the solvent, was obtained in the measurements of the kinetics of oxygen binding to cobalt(II) lacunar cyclidenes.[13,14] These observations permit comparison of experimental results on dioxygen affinities of five-coordinate cyclidene complexes measured in acetonitrile with the computational modeling of solvation of the same complexes in methanol. The dioxygen affinity of planar Co([14]Cyc) has not been measured, because of complications due to competing autoxidation processes.

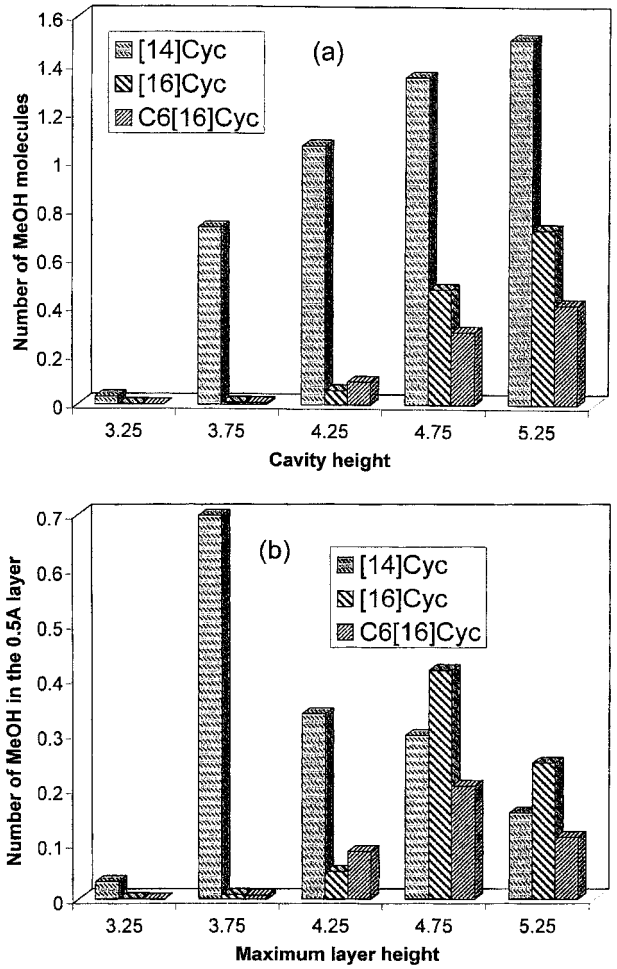

Figure 12. (a) Number of methanol molecules (calculated as MeOH center of mass) within a macrocyclic cavity of a given height. The cavity was defined as a parallelogram with a square base with a 6.5 Å side, oriented in the $Co(N_4)$ plane. (b) Number of methanol molecules (calculated as MeOH center of mass) within 0.5 Å layers crossing the cavity parallel to the $Co(N_4)$ plane. The maximum distance from the Co atom is shown for each layer, i.e., 3.75 Å on the graph corresponds to the layer spreading from 3.25 to 3.75 Å.

The UV−visible absorbance changes upon oxygenation of Co([16]Cyc) were completely reversible and typical of the formation of cobalt(II) cyclidene dioxygen adducts.[12,64] $K(O_2)$ values were calculated by fitting the experimental absorbance changes to the Ketelaar equation.[74] The dioxygen affinities obtained in pure acetonitrile and in acetonitrile/MeIm are summarized in Table 3. As expected, the $K(O_2)$ values measured in acetonitrile are much lower than the dioxygen affinities of the same complex in the presence of an axial base, 1-methylimidazole. Similar $K(O_2)$ values were obtained earlier for the bridged complex, Co(C6[16]Cyc).[1,12,75]

(73) It should be noted that the oxygen atoms of the methanol molecules were used to represent a radial solvent distribution around the Co center, while the centers of mass of methanol molecules were used to count the solvent molecules within the cavity. This difference accounts for seemingly different Co−solvent distances in these two types of distributions.

(74) Ketelaar, J. A. A.; Van de Stolpe, C.; Gouldsmit, A.; Oskubaz, W. *Recl. Trav. Chim. Pays-Bas* **1952**, *71*, 1104.

Table 3. Thermodynamic Parameters for Oxygenation of 16-Membered Co(II) Cyclidene Complexes

T, °C	$K(O_2)$, $Torr^{-1}$	ΔH, kcal/mol	ΔS, eu[a]
	Co([16]Cyc)(MeIm), in 0.0125 M MeIm/CH_3CN		
0.0	0.132(3)	−8.2	−34.0
15.0	0.061(2)		
20.0	0.049(4)		
25.0	0.036(2)		
	Co([16]Cyc), in CH_3CN		
−5.0	0.0063(8)	−7.7	−48.4
5.0	0.0041(6)		
15.0	0.0025(4)		
25.0	0.0015(5)		
	Co(C6[16]Cyc)(MeIm), in 1.5 M MeIm/CH_3CN (refs 1, 12)		
−10.1	4.6	−17.2	−63.1
1.0	1.3		
2.1	0.98		
15.0	0.25		
20.0	0.155		
	Co(C6[16]Cyc), in CH_3CN (refs 1, 12)		
−34.4	0.062	−11.8	−54.8
−27.5	0.043		
−20.0	0.026		
−10.2	0.006		
−4.8	0.005		

[a] Standard state: 1 Torr.

The analysis of the temperature dependencies of the $K(O_2)$ values, however, reveals substantial differences between the C6-bridged complex and its unbridged analogue. The values for the enthalpy and entropy of dioxygen binding were calculated from linear van't Hoff plots. The enthalpy of O_2 binding to Co(C6[16]Cyc)(MeIm) (−17.2 kcal/mol[1,12]) is substantially lower, and larger in absolute value than the corresponding ΔH value for dioxygen binding to unbridged Co([16]Cyc)(MeIm) (−8.2 kcal/mol). Contrary to the changes in ΔH, the entropy change is less unfavorable for the oxygenation of the unbridged complex (Table 3). This compensation effect accounts for the similar $K(O_2)$ values obtained for the two complexes at room temperature. These thermodynamic changes are consistent with a five-coordinate structure in the CH_3CN−MeIm solution in the case of the C6-bridged complex, and with a six-coordinate structure (with an extra solvent or base molecule coordinated to the cobalt(II) center) in the case of the unbridged complex. The dissociation of the sixth ligand would cause some relative enthalpy loss upon oxygen adduct formation, while partially canceling the loss in translational degrees of freedom associated with dioxygen binding.

However, the results of previous ESR and electrochemical studies indicate strongly that the unbridged 16-membered cobalt(II) cyclidene complex has a low-spin, five-coordinate structure both in the absence and in the presence of 1-methylimidazole.[50,76] If competitive binding to the cobalt center is not involved, then an alternative explanation is required. Accordingly, it is suggested that the solvent crowds the binding site and makes it difficult to bind dioxygen in the case of the unbridged 16-membered cobalt(II) cyclidene complex. This suggestion supports Collman's "solvent shielding" hypothesis, first proposed for small molecule binding to sterically hindered porphyrins (Figure 1).[21,22] The results of our simulations provide a microscopic view of this solvent crowding in cyclidene complexes, with the solvent molecules blocking the entrance into the cavity. Solvation of the unbridged Co([16]Cyc)(MeIm) complex is more extensive than solvation of the lacunar complex Co(C6[16]Cyc)(MeIm), and the solvent (noncoordinated) sterically interferes with dioxygen binding. Desolvation is therefore necessary for the oxygenation of the unbridged complex, limiting the magnitude of the negative enthalpy change upon oxygenation, and partially compensating for the unfavorable entropy change accompanying oxygen binding. This effect is expected to be even more pronounced for the planar unbridged 14-membered cyclidenes.

Similar arguments can be used for the interpretation of our kinetic data on the dynamics of oxygen binding.[13,14,24] For the 16-membered cyclidene complexes, unbridged Co([16]Cyc)(MeIm) reacts with O_2 about 5 times slower than with the best of the bridged complexes, Co(C8[16]Cyc)(MeIm).[14] As has been discussed above, both unbridged and bridged 16-membered cyclidenes preferentially exist in saddle-shaped conformations, and the cobalt(II) center is not extensively solvated in these complexes. Some difference in solvation at distances of ca. 4−5 Å from the cobalt atom may contribute to differences in their oxygenation rates. For a different class of cobalt(II) oxygen carriers, pentadentate Schiff base ligands, the difference in oxygenation rates between unbridged and bridged complexes is significantly greater (about 100-fold).[24] In this case, the unbridged complex does not exist in a saddle-shaped conformation, and extensive solvation of a cobalt(II) center is expected, by analogy with planar cyclidene Co([14]Cyc). This nonspecific solvation of a metal coordination site may account for much slower oxygenation of the unbridged complex with a pentadentate Schiff base ligand, as compared to the bridged ligand with a sterically protected cobalt(II) coordination site.

Conclusions

Molecular dynamics simulations of three five-coordinate cobalt(II) complexes in methanol solution revealed distinctly different solvation patterns for these complexes of different molecular shapes. While the planar 14-membered macrocycle Co([14]Cyc) is extensively solvated, with one of the solvent molecules being positioned right above the metal center at a short distance of about 2.5 Å, saddle-shaped 16-membered complexes Co([16]Cyc) and Co(C6[16]Cyc) have no solvent molecules close to the metal ion. Some solvent density is present, however, at the entries into the cleft in the unbridged complex Co([16]Cyc). The bridge in the lacunar Co(C6[16]Cyc) provides further protection of the metal coordination site from the solvent. It is important to note that no chemical bond between the cobalt atom and the methanol oxygen atom was imposed on any of the investigated systems.

The overall macrocycle geometry of each of the complexes studied does not change significantly in the course of 200 ps simulations. For unbridged complexes Co([14]Cyc) and Co([16]Cyc), the presence of a solvent (methanol) in the simulations did not influence the cavity size and other geometric parameters of the complexes. In case of bridged complex Co(C6[16]Cyc), the average cavity width in methanol simulations is about 0.3 Å smaller than in a vacuum. Most likely, this effect is caused by solvation from outside the empty cavity. This cavity shrinking in the solvent is unusual; to the extent of our knowledge, no similar examples have been reported.

Different solvent structure in the vicinity of a vacant cobalt(II) coordination site is reflected in different reactivity toward small molecules of the cobalt(II) center. This has been demonstrated in the experimental studies of dioxygen affinity of

(75) Tweedy, H. E.; Alcock, N. W.; Matsumoto, N.; Padolick, P. A.; Stephenson, N. A.; Busch, D. H. *Inorg. Chem.* **1990**, *29*, 616.
(76) Deng, Y. Dioxygen binding properties of the cobalt(II) cyclidene complexes and their catalytic oxygenation reactions. Ph.D. Thesis, The Ohio State University, Columbus, OH, 1991, 183 pp.

16-membered cyclidenes. Earlier kinetic studies of dioxygen binding to cobalt(II) complexes can also be interpreted in terms of differences in the solvation of differently shaped molecules, which competes with oxygenation to different extents.

The results of this study are not limited to a specific class of cyclidene complexes, but should be applicable to a wide range of systems with steric hindrance around a metal ion coordination site, including metalloenzymes and their synthetic models.

Acknowledgment. This work has been supported by the NSF under Grant No. 9550487 and matching support from the state of Kansas. The authors gratefully acknowledge the University of Kansas Molecular Modeling and Graphics Laboratory for making available their computer resources for a part of this project. We thank Professor Nathaniel W. Alcock for providing the X-ray coordinates for several cyclidene complexes in a computer readable format and Dr. Ann Hermone for providing CHARMM force field parameter file for retinal.

Supporting Information Available: A figure showing complete atom numbering schemes and CHARMM topology and force field parameter listings. This material is available free of charge via the Internet at http://pubs.acs.org.

IC9904485